IRWIN AND JOAN JACOBS
CENTER FOR COMMUNICATION AND INFORMATION TECHNOLOGIES

High Numerical Aperture Singular Beam Scanning Microscopy: Preliminary Experimental Results

Boris Spektor, Alexander Normatov and Joseph Shamir

CCIT Report #727
May 2009

DEPARTMENT OF ELECTRICAL ENGINEERING
TECHNION - ISRAEL INSTITUTE OF TECHNOLOGY, HAIFA 32000, ISRAEL

CCIT REPORT #727 May 2009

High numerical aperture singular beam scanning microscopy: preliminary experimental results

Boris Spektor, Alexander Normatov*, Joseph Shamir
Technion – Israeli Institute of Technology; Technion City, Haifa 32000, Israel

ABSTRACT

High sensitivity and a high speed nanoscale measurement becomes an important subject in modern industry, when analysis of high speed moving nanoscale objects on a surface is required. Recently we have shown a possible approach to this problem using singular beam microscopy. Singular beam microscopy performs scanning by utilization of the relative movement between the focused singular beam and the investigated object. This allows collection of sufficient information for evaluation of various features of the investigated object. Our theoretical results were in good agreement with the experimental results, which showed 20nm experimentally proven sensitivity under a moderate numerical aperture of 0.4. One of the possibilities for sensitivity improvement is increasing the numerical aperture. In this publication we report our progress with a numerical aperture of 0.55. This transition requires rigorous numerical analysis and a more accurate experimental setup. In order to approach the problem of modeling tight singular beam focusing, we developed an extension of the existing Richards-Wolf method which allows evaluation of a 3D tightly focused optical field. The modeling of scattering of tightly focused singular beams can be done by existing electro-magnetic methods. In this work we will present experimental results of detection and evaluation of a phase step in different experimental conditions. The investigated equivalent phase step heights were down to 10nm.

Keywords: Singular beam, nano-scale, focusing, high-NA

1. INTRODUCTION

Methods for characterizing geometrical and optical properties of nanoscale objects and features receive much attention in the present decade. This interest is justified by the importance of these methods in nanotechnology and related industries. Recently we suggested a promising method, capable of nano-metric sensitivity at sufficiently long working distance[1]. The suggested method allows both, high speed and a high sensitivity, by trading off some aspects, which are less important for industrial applications. This method demonstrated experimental sensitivity of 20nm for a moderate numerical aperture (NA) of 0.4 while paraxial numerical analysis predicted capability of an order of 1nm sensitivity for a reasonable optical system signal to noise ratio of 30dB. A good correlation between the experimental results and corresponding numerical simulations was observed.

The performance and capabilities of the suggested scanning microscopy method can be extended further in a number of ways. Increasing the NA of the optical system can produce higher localization of the scanning beam and thus improve the sensitivity. Unfortunately, increasing the NA places more stringent experimental and practical requirements on the optical system and the measurement procedure and requires a much more complex analysis than the one needed for lower numerical apertures. Extension of the analysis to 3D presents an additional analytical and numerical challenge.. The suggested method was initially demonstrated on a phase step[1,2,3] but in practice, other types of nanoscale objects should be investigated as well. An interesting option for an extension of the original method is utilizing other types of structured illumination. The aim of this publication is a summary of recent advances in the field of scanning singular beam microscopy both analytical and experimental. This paper is organized as follows. The next section is dedicated to a short description of high NA scanning singular beam microscopy and related rigorous analysis. Section 3 reports on our progress with NA=0.55. Finally, conclusions are drawn.

*alexn@tx.technion.ac.il; phone +972-4-8294702; fax +972-4-829-5757;

2. OVERVIEW AND RIGOROUS ANALYSIS

2.1 General optical system

A detailed description of a SB scanning system is given in Ref. 1. In this section we discuss a corresponding high NA optical system and its analysis. We start with a plane wave, generated elsewhere, that passes through a phase mask, situated immediately before the entrance pupil of an optical system as shown in Fig. 1. Thus we can introduce a piecewise quasi constant phase[4] in the incident wavefront. The addition of this phase allows embedding some types of optical singularities.[5] This wavefront enters the optical system in the direction of the optical axis, z. The high NA optical system focuses it at its back focal plane.[6] At the back focal plane, in the vicinity of the geometrical focus O, the tightly focused beam is scattered by a nanoscale object. At present we are concerned with forward scattering in the direction of *z*. The light intensity resulting from the superposition of the incident and the scattered fields is recorded at the recording plane. This plane is situated at a distance *d* from the back focal plane of the optical system which is adequately large to be considered as the far zone. For each position along the scan of the investigated object the resulting intensity is recorded. Analysis of the recorded scattering results, together with some *a priori* information about the object, enables the evaluation of nanoscale features of the object.

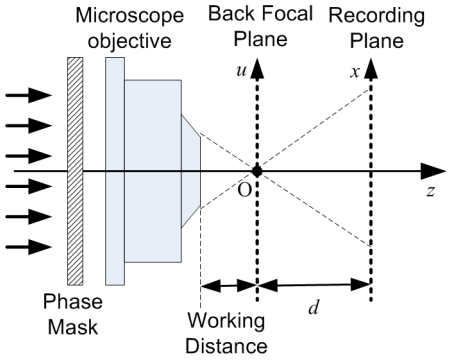

Fig. 1. Schematic diagram of the optical system. A plane wave passes through a phase mask, located immediately before the entrance pupil of the focusing lens. The focused wavefront is evaluated at the back focal plane, where the investigated object is situated. In the process of investigation the objects is scanned by the focused beam. The light scattered by the object in the forward propagation direction is measured at the recording plane.

2.2 Rigorous analysis

High numerical aperture focusing analysis methods are based on the Richards-Wolf (RW) approach.[7] A review of these methods is given in Ref. 4. Yet, all these methods assume that the wavefront, incident on the entrance pupil, is planar or has very slow phase variations. Analysis of some types of the tightly focused SB required the adaptation of the existing methods to wavefronts having piecewise quasi constant phase.[4] Our extension of the RW approach[7] is based on the fact that the Debye-Wolf integral[8] represents a superposition of individual rays originating at the incident wavefront. The above approach holds when the incident wavefront can be adequately represented by rays parallel to the optical axis. This allows division of the incident wavefront into a finite number of quasi constant phase segments. Assuming that only a small fraction of the energy in the incident field is contained in regions where non-negligible phase variations occur, we modified the integral to allow the summation of rays having different relative phases, corresponding to the different segments. The numerical evaluation of the summation produces a tightly focused field corresponding to the applied boundary conditions. In our work[4] we also studied the influence of the boundaries between neighboring constant phase segments. Using our method[4] we made an analysis of focal field distributions for various illumination cases.[9]

The tightly focused field, evaluated according to the above, is incident on the investigated object. For each scan position between the focused beam and the object a scattering analysis should be performed. Scattering from certain objects, like spheres or conducting half planes can be performed analytically, provided the focused incident wavefront has a convenient representation as a plane wave spectrum.[10] Scattering from other objects usually requires numerical approach. Due to a high complexity of a scattering problem, it is important to select an appropriate method, based on the problem geometry, object properties, incident illumination, required accuracy and available resources. Various approaches, like Finite Element Method,[11] Rigorous Coupled Wave Analysis[12] and others are discussed in Ref. 6.

Scattering analysis usually yields fields in the vicinity of the scattering object. The propagation of these fields to the far zone is usually accomplished by the Stratton-Chu[13] (SC) integration of the near field. Such calculation is straightforward when only the scattered component of the far field is required. In the case of scanning microscopy, the measured quantity is the intensity of the total far field. This field has both the contribution of the scattered field and the contribution of the incident focused field. In some cases, when the far field contribution of the focused field is known (like for Gaussian beams), then the total far field can be immediately obtained as a coherent sum with the scattered far field. In other cases the evaluation of this field is not trivial. The issues related to the far field evaluation are discussed in Ref. 6.

When the NA of the optical system is not too high and the investigated objects are large enough, it is possible to resort to paraxial analysis methods. In this case, the reduction of accuracy is traded off by evaluation time. Recently we performed an investigation of the influence of the shape of various scattering objects having the same phase volume[14]. The results suggest that extraction of the shape information requires an order of magnitude higher sensitivity than the one needed just for estimation of the phase volume.

3. EXPERIMENTAL RESULTS

This part of the publication is dedicated to demonstration of preliminary experimental results obtained with phase step objects of significantly smaller value than earlier published results. Unfortunately, various limitations, like the complexity of the involved electro-optical system prevented a proper experimental coverage. Therefore, the presented results should not be compared or evaluated quantitatively. Their sole purpose is a proof of concept and a qualitative impression of the involved signal to noise ratio and corresponding sensitivity.

3.1 Experimental optical system

The experimental optical system, having NA=0.55 and 532nm – second harmonic of Nd:YAG laser, is conceptually similar to the one presented in Fig. 1. Yet, there is a number of important differences. First, the wavefront, incident on the microscope objective, is already a dark beam[1,15] (DB) generated at a preceding stage. Thus the idealized singular beam generation by a plane wave does not take place like shown in Fig. 1. In real experimental setup the DB was generated involving spatial filtering procedures in order to get an apodized form of a DB at the focal plane for removal of side-lobes. Certainly, the focused beam in the experimental case is different from the one evaluated numerically. Moreover, at this stage, rigorous evaluation of the tightly focused DB, based on experimental procedure, involves making significant approximations that degrade the accuracy, and therefore is not reliable.

The second difference is the structure of the scattering object. In the ideal case, the object is a dielectric fixed in a free space. In practice, the phase step is etched in a glass substrate. The substrate with an etched phase step is placed in a quartz cell. In order to check the detectability of the lower phase step values, the cell is filled with ethanol. The described environment affects the way the light is focused[16] and the way it propagates after being scattered. Modeling of this environment requires a great analytical and numerical effort before any compatible results can be obtained.

Finally, the intensity recording is performed by photo-detectors placed in specific regions in the far field. The system includes collecting of the scattered light by a lens placed in the far field, diffusing the collected light by a diffuser for reduction of influence of coherence effects, collecting the light by a photo-detector and registering the resulting intensity by an oscilloscope.

Two different phase steps were used. Both were made by wet etching a glass substrate. The smaller step was about 50nm high and the bigger was about 80nm high. The equivalent phase delay of a step can be calculated as:

$$\Delta\phi = 2\pi \frac{\left(n_{step} - n_{env}\right)h}{\lambda} \tag{1}$$

Where n_{step} is the refractive index of the material of the step (taken as 1.49 for glass), n_{env} is the refractive index of the surrounding environment (for air it is taken as 1 and for ethanol it is taken as 1.36242), h is a step height and λ is the illumination wavelength. When placed in air, the above phase steps produce phase delays of approximately: 0.289rad and 0.463rad. In the course of the experiments, it was important to investigate the response to very small values of the phase step delay. For this reason the investigated step was placed in a quartz cell and the cell was filled with ethanol. As

the refractive index of ethanol is higher than that of air, the corresponding phase delays were approximately: 0.0753rad and 0.1205rad. An equivalent phase step height for obtaining these phase delays in air can be obtained from (1) as:

$$h = \frac{\lambda \Delta \phi}{2\pi \left(n_{step} - n_{env} \right)} \tag{1}$$

On making the calculation, the following equivalent approximate heights are obtained: 13nm and 20nm.

A number of additional difficulties can be pointed out. The fabrication of the phase step, performed by etching, produces a rough surface at the etched part. Moreover, the etching is deeper in the immediate vicinity of the step as compared to the overall etched surface level. Precision measurements of the phase step profile yielded that the actual height of the step was not uniform. The variations for the phase step height, for a phase step referred here as 50nm, were between 35nm and 55nm. Thus the equivalent phase step heights can be evaluated between 9nm and 14nm.

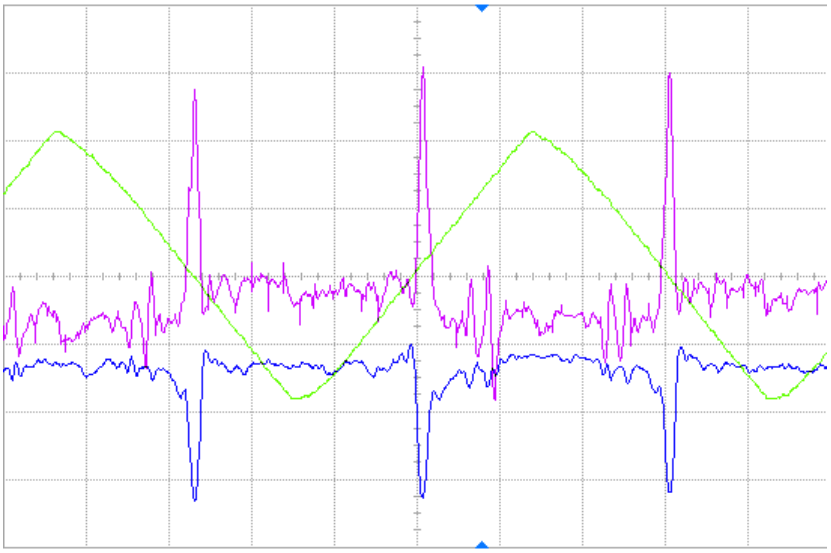

Fig. 2. Response of a 50nm phase step in air. The upper curve represents the readout of a photo detector in the forward scattering direction and the bottom curve corresponds to back scattering direction. The vertical resolution is 20mV/division. The relative position of the phase step to the focused illumination is represented by a triangular signal, having amplitude of 20 microns.

3.2 Results and discussion

An experimental result involving a phase step of 50nm in air is shown in Fig. 2. The triangular signal represents the output of the nano-positioning stage, reflecting the movement of the phase step. In this figure the amplitude of the movement was 20 microns. The output of the photo detector situated in the scattering direction corresponding to forward propagation (i.e. in the positive direction of *z* axis in Fig. 1) is represented by the upper curve. The reading from a photo detector situated in the back scattering direction (i.e. in the negative direction of *z*) is represented by the bottom curve. The signals exhibit mirror-like symmetry around the extreme points of the triangular signal. This is due to periodical bidirectional movement of the phase step relative to the focused spot. The upper curve peaks rise some 60mV above the average level, while those of the bottom curve plunge about 30mV below the average level. It should be noted that the absolute values of the peaks have no meaning as they depend on many parameters in the system, like laser power, amplification of the photo detector signal, exact photo detector positioning, etc. The height of these peaks should only be viewed relative to the form and fluctuations of the signal between the peaks. Such relation gives a perception of achievable signal to noise ratio of the measurements. The noisy fluctuations between the peaks are caused by laser power instability and surface roughness left from the wet etching procedure as can be seen in Fig. 2. A part of this noise, caused by laser power instability can be suppressed by averaging as will be shown, for example, in Fig. 4.

In a similar way, Fig. 3 shows the response for the 80nm phase step in air. Only the forward scattering response is presented. Due to the differences in setup, the signal has now both positive and negative peaks while for the 50nm case there were only positive or negative peaks. These differences, among others, include positioning of the detector and orientation of the phase step. In Fig. 4, some setup similar to that of Fig. 3, is used. The recorded signal is an average of 64 consecutive measurements. The waveform in Fig. 4 has much smoother shape than those in Figs. 2, 3 and it has a distinct repetitive form.

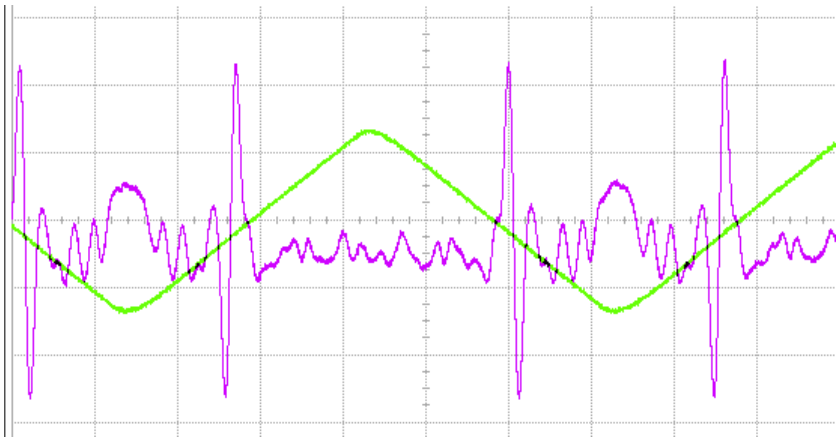

Fig. 3. Response of an 80nm phase step in air for forward scattering. The vertical resolution is 200mV/division. The relative position of the phase step to the focused illumination is represented by a triangular signal, having amplitude of 15 microns.

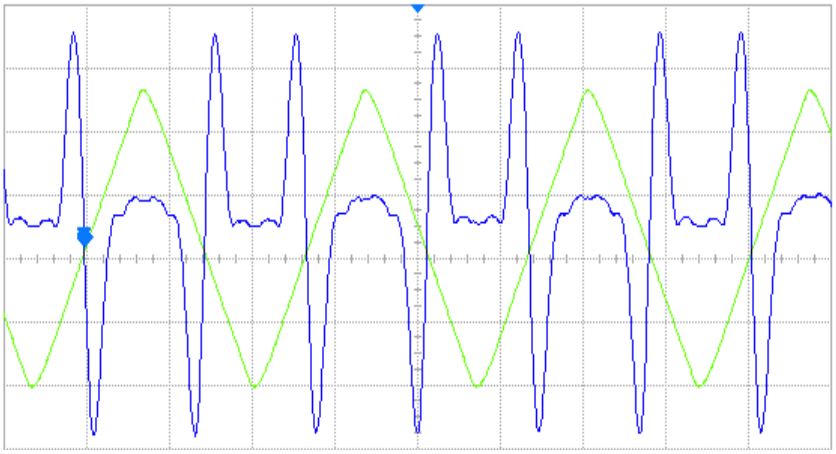

Fig. 4. Response of an 80nm phase step in air for forward scattering. The vertical resolution is 20mV/division. The relative position of the phase step to the focused illumination is represented by a triangular signal, having amplitude of about 12 microns. The signal represents average of 64 measurements.

We now turn to results obtained with the same phase steps immersed in ethanol. The results for 80nm phase step are shown in Fig. 5. A high degree of similarity between the two signals is apparent. The difference of signal amplitude in milli-volts is not representative, as the different setups used in these experiments included different laser power levels and different levels of amplification of the photo detector.

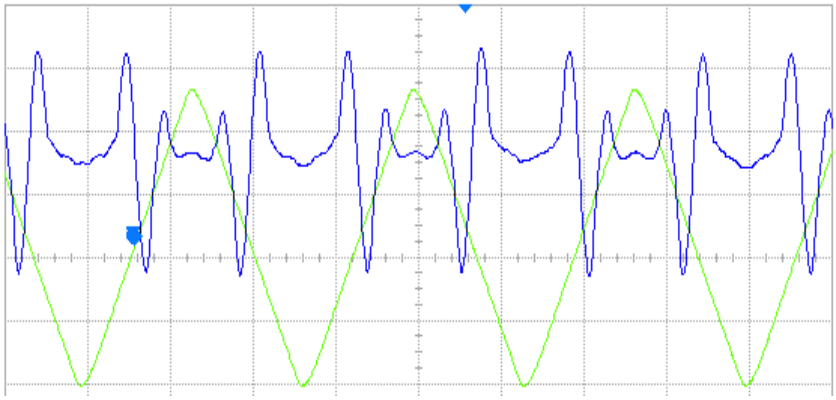

Fig. 5. Response of an 80nm phase step in ethanol for forward scattering. The vertical resolution is 20mV/division. The relative position of the phase step to the focused illumination is represented by a triangular signal, having amplitude of about 12 microns. The signal represents average of 64 measurements.

In a slightly different setup, the response of 80nm phase step, immersed in ethanol, was measured both in the forward scattering direction and in the back scattering direction. The results are presented in Fig. 6.

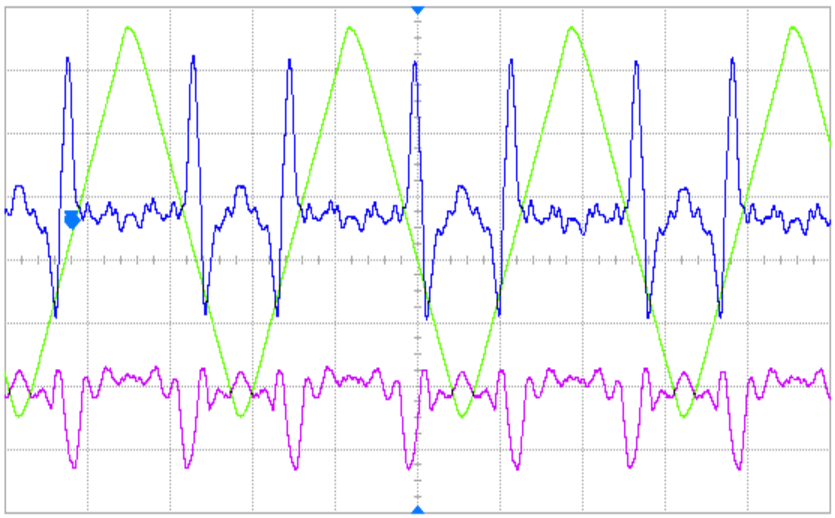

Fig. 6. Response of an 80nm phase step in ethanol. The upper curve represents the readout of a photo detector in forward scattering direction and the bottom curve corresponds to back scattering direction. The vertical resolution of the upper curve is 100mV/division, for the bottom curve it is 50 mV/division. The relative position of the phase step to the focused illumination is represented by a triangular signal, having amplitude of 15 microns. The signal represents average of 64 measurements.

The immersion results for 80nm correspond to an equivalent phase step of 22nm in air, as calculated before. Lower equivalent value, of below 14nm phase step in air, is obtained by working with immersed 50nm step. The result for 50nm phase step immersed in ethanol is shown in Fig. 7. As previously, for the 50nm step we get single peaks instead of double peaks of the 80nm sample.

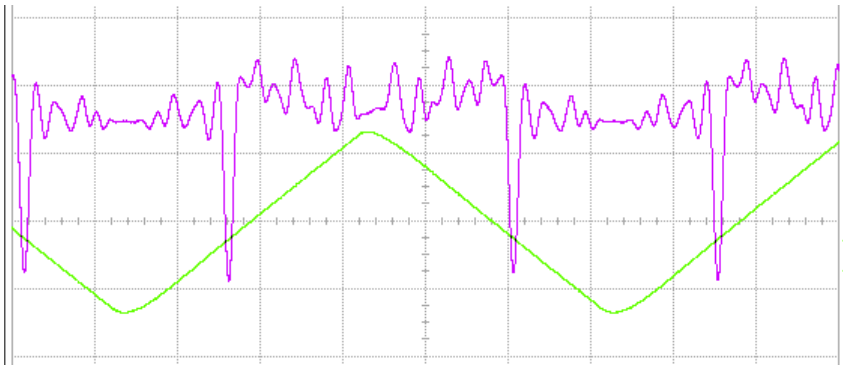

Fig. 7. Response of a 50nm phase step in ethanol for forward scattering. The vertical resolution is 50mV/division. The relative position of the phase step to the focused illumination is represented by a triangular signal, having amplitude of about 15 microns. The signal represents average of 64 measurements.

4. CONCLUSIONS

In this work we presented an overview of the latest achievements in the field of singular beam microscopy as well as the description of the current challenges. We discussed both the analytical part and experimental part. Unfortunately, at the current stage, it was not possible to make a meaningful comparison between analytical and experimental results. In spite of the described challenges and difficulties, the presented preliminary experimental results prove that phase step structures with heights down to 10nm can be successfully detected with sufficient signal to noise ratio. A qualitative estimation of the achievable signal to noise ratio is impressive when considering modest investigation system parameters.

Acknowledgements

This work was performed within the NANOPRIM project supported by the European Community under the FP6 program. The authors thank V. Golobordko for his valuable help in conducting the experimental investigations.

REFERENCES

[1] Spektor, B., Normatov, A. and Shamir, J., "Singular Beam Microscopy," Appl. Opt. 47(4), A78-A87 (2008).
[2] Normatov, A., Spektor, B. and Shamir, J., "Capabilities and limitations of paraxial operator approach for modeling of nano-scale feature evaluation", Proc. SPIE 6617, 661704 (2007).
[3] Spektor, B., Normatov, A. and Shamir, J., "Experimental validation of 20nm sensitivity of singular beam microscopy", Proc. SPIE 6616, 661622 (2007).
[4] Normatov, A., Spektor, B. and Shamir, J., "Tight focusing of wavefronts with piecewise quasi-constant phase", Opt. Eng. 48, 028001 (2009).
[5] Nye, J. F. and Berry, M. V., "Dislocations in Wave Trains", Proc. R. Soc. Lond. A. 336(1605), 165-190 (1974).
[6] Normatov, A., Spektor, B. and Shamir, J., "Numerical analysis of tight focusing and scattering of singular beams", Proc. IEEE 25th Convention of Electrical and Electronics Engineers in Israel, IEEEI 2008, 66-69 (2008).
[7] Richards, B. and Wolf, E., "Electromagnetic diffraction in optical systems, II Structure of the image field in an optical system," Proc. R. Soc. Lond. A. 253(1274), 358-379 (1959).
[8] Wolf, E., "Electromagnetic diffraction in optical systems, I An integral representation of the image field," Proc. R. Soc. Lond. A. 253(1274), 349-357 (1959).
[9] Normatov, A., Spektor, B. and Shamir, J., "High numerical aperture focusing of singular beams", Proc. SPIE 7227, 722709 (2009).
[10] Born, M. and Wolf, E., [Principles of Optics], Cambridge University Press, (2003).
[11] Jin, J., [The Finite Element Method in Electromagnetics], Wiley, (1993).

[12] Moharam, M. G. and Gaylord, T. K., “Diffraction analysis of dielectric surface-relief gratings,” J. Opt. Soc. Am., 72(10), 1385-1392 (1982).
[13] Stratton, J. A. and Chu, L. J., “Diffraction Theory of Electromagnetic Waves,” Phys. Rev., 56, 99-107 (1939).
[14] Normatov, A. and Spektor, B., are working on a manuscript called “Nanoshaped objects of equal phase volume: scattered far field comparison” accepted to presentation at SPIE Europe Optical Metrology conference.
[15] Spektor, B., Piestun, R. and Shamir, J., "Dark Beams with a constant notch," Opt. Lett. 21(7), 456-458 (1996).
[16] Torok, P., Varga, P., Laczik, Z. and Booker, G. R., “Electromagnetic diffraction of light focused through a planar interface between materials of mismatched refractive indices: an integral representation”, J. Opt. Soc. Am. A. 12(2), 325-332 (1995).